Bull. Iraq nat. Hist. Mus.
(2021) 16 (3): 301-323. https://doi.org/10.26842/binhm.7.2021.16.3.0301

ORE GENESIS AND MINOR ELEMENTS OF OROGENIC GOLD DEPOSIT AT TAMILOUW– HAYA, SERAM ISLAND, INDONESIA

Herfien Samalehu* Arifudin Idrus**♦ Nugroho Imam Setiawan**
and
I Gede Sukadana***

* Energy and Mineral Resources Agency, Maluku Province, Indonesia.
**Department of Geological Engineering, Universitas Gadjah Mada, Yogyakarta, Indonesia.
***National Atomic agency, Indonesia.
♦Corresponding author: arifidrus@ugm.ac.id

Received Date: 05 March 2021, Accepted Date: 30 April 2021, Published Date: 20 Jun 2021

ABSTRACT

The orogenic gold deposit of Tamilouw – Haya is hosted by slate and metapelitic rocks within Tehoru metamorphic complex. Gold and polymetallic sulfides mineralization at study area is predominantly formed in the form of veins, stockwork and breccia although minor dissemination is slightly appeared in the rock float samples. They are trapped and controlled by NE-SW and NNE-SSW trending geologic structure occurred during orogeny process from Late Miocene to Pliocene. The common ore minerals assemblage at Tamilouw – Haya deposit are dominated by native gold, chalcopyrite, pyrite, sphalerite, galena, pyrrhotite, tetrahedrite-tennantite (sulphosalt), marcasite,realgar, kalininite and arsenopyrite as hypogene minerals and accompanied by covellite, hematite, goethite and malachite as the supergene minerals.

Ore genesis and minor elements study of pyrite, galena, and sphalerite at Tamilouw – Haya was done using 3 methods approach. There were 46 samples used for ore microscopy analysis and 10 samples for SEM-EDX and Micro-XRF analyses to obtain their mutual relationship interpretation and paragenetic sequence. Ore mineral textures showed disseminated textures, simultaneous crystallization (intergrowth), inclusions, replacements, and exsolutions-decomposition textures.

Average content of Co is 0.21 wt. % and Ni is 0.10 wt. % which may reflect the Co : Ni ratio is 2.86 in pyrite. It means that Co content is higher than Ni and indicates that pyrite origin may be related to volcano-hydrothermal, metamorphosed and skarn-hydrothermal type. In comparison with pyrite, the average contents of minor elements in sphalerite shows Fe content is 9.16 wt.%, Ga is 0.99 wt.%, Ge is 0.12 wt.% and log Ga/Ge ranging from < 0.36 to 2.27 wt.%. Moreover, average precious metal contents within galena shows that Au contents is < 0.01 – 2.78 wt.% and Ag is 0.12-0.31 wt.%. On the basis of the previous descriptions, high content of Fe in pyrite and sphalerite, Ga > Ge, Co > Ni in pyrite and low content of Ag in Galena indicated that pyrite, galena, and sphalerite from Tamilouw – Haya were formed under high to moderate temperature condition at 5.1-7.6 km paleodepth.

Keywords: Gold, Metamorphic, Mineralization, Orogenic, Seram.

INTRODUCTION

Bierlein *et al*. (2001) revealed that Orogenic gold deposits are related to collision settings and active orogenic belts. These deposit are formed during compressional to transpressional regimes at convergent plate margins both accretionary and collisional orogens (Groves *et al.*, 1998; Goldfarb *et al*., 2001, 2015). They are epigenetic, structurally controlled and based on their depth of formation; they are divided into epizonal, mesozonal, and hypozonal (Groves *et al*., 1998; Goldfarb *et al.*, 2005).

In Indonesia, many researchers had investigated the occurrence of gold mineralization within metasediments to metamorphic rocks formation. Some large and medium scale of gold deposits such as Awak mas mesothermal (Querubin and Walters, 2011), Poboya LS – Epithermal (Wajdi *et al*., 2011), Bombana orogenic gold deposits (Idrus and Prihatmoko, 2011), Buru orogenic Gold deposits (Idrus *et al*., 2014), Mendoke - Rumbia orogenic gold (Hasria, 2018) and many gold mineralizing occurrences were successively discovered in indonesia. Except for the Tamilouw – Haya gold deposits, which are located in the southern part of Tehoru Metamorphic complex, there were no major orogenic gold deposits that have been recognised in Seram Island yet. Nevertheless, several gold occurrences have recently been identified in the western part of Seram and a previous study of metamorphic rock - hosted gold mineralization was proposed for prospecting only with no classification of ore genesis deposit type and their genetic model (Franklin *et al*., 2013).

Seram Island is located along the northern part of outer Banda arc, eastern Indonesia. It is previously located in the collision zone between Australian Continent and Banda Subduction Zone, where the Northwest Australian margin moved towards Banda Subduction Zone. The Northwest shelf of Australia itself was generated due to the break-up of Gondwana during Jurassic (Powell, 1976; Veevers, 1982).

Stratigraphically, Seram can be divided into two parts; Australian series and Seram series (Map 1A). A northern belt, covering the north part of the island in the west and all of it in the east, consists of imbricates sedimentary rocks of Triassic to Miocene age (Australian series) whose fossils and facies resemble those of the Misool and New Guinea continental shelf (Hamilton, 1979). These sedimentary formations, i.e., Kanikeh Formation, Saman-Saman limestone, Manusela Formation, Lisabata Formation and Salas block clay; others sedimentary rocks formations named Fufa and Wahai formations are classified as Seram Series. The southern belt is dominated by metamorphic rocks with the basement consists of high to low grade metamorphic rocks. The high-grade metamorphosed schists and gneisses of the Kobipoto Complex are probably Precambrian to Lower Palaeozoic, although the recent study argued its formation aged Late Miocene to Pliocene (Pownall *et al*., 2013). Other Palaeozoic rocks are Taunusa, Tehoru and Saku complexes (Tjokrosapoetro *et al.*, 1993).

Center and western Seram mainly comprises of lower greenschist to upper-amphibolite facies, i.e., phyllites, schists, and gneisses of the Tehoru formation. Garnet micaschists are widespread, which are often intercalated with amphibolites. Scarce kyanite-grade schists represent the highest grade part of the complex; however, large areas are of a low metamorphic grade and preserve original sedimentary structures (Audley-Charles, 1979; Tjokrosapoetro and Budhitrisna, 1982; Linthout *et al*., 1989). The Taunusa Complex is very similar in many ways to the Tehoru Formation although it includes rocks previously assigned to Valk (1945) as “Crystalline Schists” and therefore is considered to be generally of higher metamorphic grade (mid/upper-amphibolite facies rather than lower-amphibolite to greenschist facies) as defined by Tjokrosapoetro and Budhitrisna (1982).

Locally, the tectonic setting of Tamilouw – haya has been influenced by regional compression of Seram Island itself; despite the tectonic setting of Seram is still subject to debate, at least there have been two times tectonic compression and two continental break-ups were related to the Seram island (Setyawan *et al*., 2000).The first continental break-up was followed by tectonic compression occurred in the Paleozoic. Subsequent contraction of earth's crust places high-grade metamorphic rocks such as granulite near the surface and upper mantle is uplifted to the surface to form ultramafic rocks. Hence, erosion occurred to further expose of these metamorphic rocks and followed by thermal subsidence as deposition of Australian series. The second continental break-up and sea floor spreading is occurred in middle Jurassic and it might correspond to the absence of sedimentation interval in the Australian series. The last orogenic compression or deformation occurred in the Late Miocene-Pliocene and this event is very critical for the geological evolution of Seram (Audley - Charles *et al*., 1979; Kemp and Mogg, 1992; Tjokosapoetro *et al*., 1993; Setyawan *et al*., 2000).

The ore mineralization process at Tamilouw - Haya is controlled by NE–SW and NNE-SSW trending geologic structure as implication of this last compression event (Map 1B). It is also notable that local geological framework indicates that the gold mineralization is probably not related to volcanic rock-related hydrothermal gold deposit, e.g. epithermal, skarn or porphyry.

The main aims of this paper are to describe and identify ore minerals assemblage and minor elements contained in pyrite, galena and sphalerite and to purpose ore forming process and their paragenetic sequence at Tamilouw- Haya, Seram Island, Indonesia.

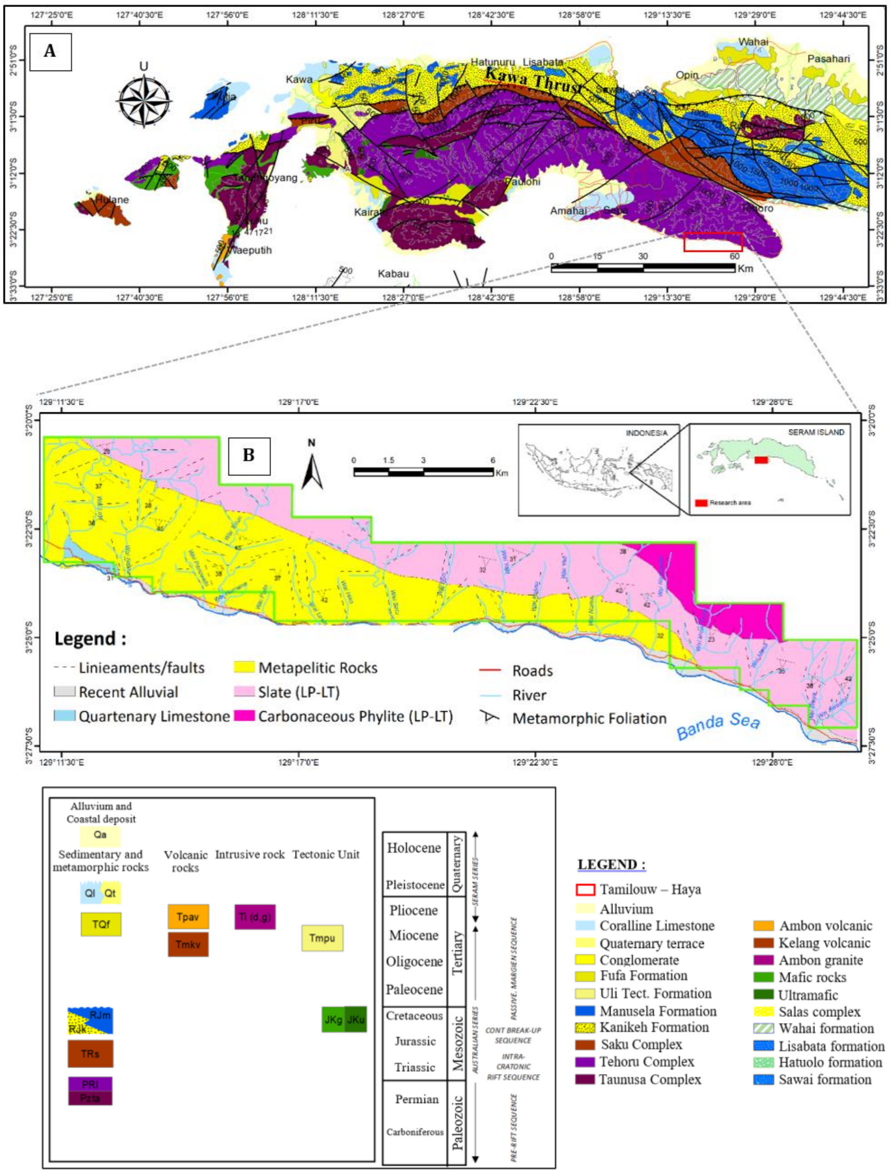

Map (1): (A) Geological map of Seram (modified after Tjokrosapoetro *et al*., 1993), (B) Simplified Geological map of Tamilouw – Haya.

MATERIALS AND METHODS

The present study is based on desk study, fieldwork and sampling for laboratory analysis i.e ore mineralogy, SEM-EDS and Micro-XRF. There is no previous detailed study in the Tamilouw - Haya area that was focused specifically on the gold mineralization. A detailed ore microscopy is conducted at Department of Geological Engineering, Universitas Gadjah Mada, a single mineral chemistry (SEM-EDS) analysis is carried out at LPPT, Universitas Gadjah Mada and Micro-XRF for mineral mapping and identification is analysed at BATAN-Jakarta.

In total 46 double polished sections were prepared for ore microscopy to identify ore minerals and their textures. There were twelve data of shoot points for pyrite, sphalerite and galena identification are based on ore microscopy observation for further elemental mapping and identification using SEM-EDX and Micro-XRF. Mineral chemistry from SEM-EDX was performed using a JSM-6510LA type with resolution 1 – 10 nm and magnification 10 – 300,000x.

MicroXRF M4Tornado plus tool at BATAN, Jakarta is used for elemental mapping and minerals identification. It was performed by tube parameter high voltage 50 Kv, anode current 600µA pixel time 25 ms/pixel, pixel size 30 µm and total number of pixel is 360,000 pixel.

RESULTS AND DISCUSSION

Tamilouw - Haya is located within Tehoru metamorphic complex, Seram Island-Indonesia. The extent of researched area is 101.46 km^2 and is predominantly occupied by metapelitic rocks (intercalated of metasandstone and metasiltstone), slate, phyllite and locally is covered by coralline limestone and recent alluvial deposit. Primary gold mineralization is hosted by slate and metapelitic rocks and controlled by NE–SW and NNE-SSW trending geologic structure. Concordant and discordant veins are associated with gold mineralization although minor disseminated type appeared in several rock float samples.

There are 6 main prospects of gold mineralization in Tamilouw – Haya area namely Wae Lata, Waenama, Wae Satu, Wae Yala, Wae namasula and Way Wayaudara. High-grade gold ores in this area is generally found in quartz±carbonate veins with the main alteration processes involving silicification, carbonatization and sericitization. Ore minerals assemblage within these veins are dominated by native gold, chalcopyrite, pyrite, sphalerite, galena, pyrrhotite, minor sulfosalts (tetrahedrite-tennantite), marcasite, realgar, kalininite and arsenopyrite.The supergene minerals are covellite, hematite, goethite and malachite.

(A) General features of ore minerals assemblage at Tamilouw – Haya

Characteristics of primary ore mineralization at Tamilouw-Haya are generally occurred within quartz veins associated with silicification, carbonatization and serisitic alterations. There are 3 vein types as the ore–bearing fluids (V_1-V_3) and only V_3 (quartz± carbonate veins) with precious metals and anomalous high basemetal contents. Concordant vein, namely quartz type 1- vein (V_1) is characterized by massive shape, sheeted, segmented, tends to parallel to the foliation of metamorphic rocks and weak mineralized to barren. Discordant veins are separated into two vein types. Quartz type 2 – vein (V_2) which is cross to the foliation, massive, weak mineralized to barren and associated with silicification and serisitic alterations.

The last, the so-called "mineralized veins" (V_3) are composed of quartz± carbonate, segmented, deformed, cross to the foliation of metamorphic/metapelitic rocks and characterized by stockwork – breccia vein textures. In some other locations, concordant veins are cross-cut by discordant veins as an indication of late stage of ore deposition. Based on ore microscopy analysis and elemental mapping, there are common ore minerals assemblage at Tamilouw – Haya deposit i.e native gold, chalcopyrite, pyrite, sphalerite, galena, pyrrhotite, tetrahedrite-tennantite (sulphosalt), marcasite, realgar, kalininite and arsenopyrite as hypogene minerals and accompanied by covellite, hematite, goethite and malachite as the supergene minerals.

Native gold: Very small size **<** 0.25 mm, subhedral – anhedral and it is found as free gold grain within quartz gangue. At Way Yala river-Tamilouw, gold is enriched by supergene process and very abundant as secondary deposit (Pl. 1A).

Pyrite: Generally euhedral – subhedral, yellow colour and very abundant as vein and disseminated texture filled in quartz gangue at Tamilouw-Haya (Pl. 1A-D). In the altered and mineralized host rock, pyrite is slightly appear as dissemination ore and accompanied by chalcopyrite. Some of pyrite replaces pyrrhotite and has an intergrowth relation with galena. In quartz gangue, chalcopyrite, sphalerite, galena and pyrrhotite show their disseminated texture.

Chalcopyrite: Bright yellow colour, size is 0.25 – 0.50 mm, subhedral – anhedral, showing ex-solution texture or blebs of chalcopyrite within sphalerite (Pl. 1D). Chalcopyrite is associated with pyrite and very abundant as disseminated texture. In some polished section, chalcopyrite is replaced by tetrahedrite and covellite (Pl. 1B).

Galena: White grey colour, specified by triangular pits, size is often > 0.25 mm (Pl. 1C). Its presence is very abundant within quartz gangue, associated with sphalerite and pyrite in intergrowth texture and occasionally appears in the disseminated texture.

Sphalerite: Grey colour, occasionally showing ex-solution texture or blebs of chalcopyrite within sphalerite or "chalcopyrite disease" (Barton and Betkhe, 1987) (Pl. 1D). Sphalerite is associated with galena and reflecting intergrowth/interlocking texture. It means that sphalerite and galena are precipitated at the same time of ore deposition. Sphalerite is in line with chalcopyrite, pyrite, pyrrhotite and galena to form disseminated texture within quartz gangue. Generally, its appearance indicates as "late stage" than others sulphide minerals.

Pyrrhotite: It is also called magnetic pyrite and recognized by brown yellow colour. The size is 0.35 – 0.5 mm of single anhedral grain. Pyrrhotite and marcasite are rare and their presence is only in quartz segregation/gangue to form disseminated texture.

Marcasite: Occasionally in shape of subhedral – anhedral, single grains, size is 0.16 - <0.32 mm and it is also called "white iron pyrite". Although marcasite is not abundant within quartz gangue, its appearance is related to disseminate texture and replaced by Fe-iron oxide (hematite).

Arsenopyrite: Grey to silver white colour, 0.5-15 mm, appears as vein/veinlets and is filling fracture/shear joints of metapelitic rocks.

Tetrahedrite: It is sulfosalt mineral, gray to dark black colour, 0.2 – 0.5 mm, tetrahedrite replacing chalcopyrite or occurred as replacement texture within quartz gangue (Pl. 1B).

Tennantite: Represent sulfosalt mineral, gray to gray black colour, 0.25 – 0.5 mm, its mutual relationship with galena is intergrowth, in some observation tennantite replaced pyrite and is substituted by hematite (Pl. 1C).

Kalininite: It is an isometric – hexoctahedral black mineral, gray to black colour, 0.05 – 0.25 mm, its appearance is associated with pyrite and hematite (Pl. 1E).

Realgar: It is a monoclinic arsenic sulfide (As_4S_4), red colour, 0.25-0.35 mm, isolated/single grains.

Covellite: Blue colour, 0.01-0.05 mm, single grain, its presence is rare within quartz gangue and only observed to replace chalcopyrite.

Hematite: It is Fe-oxide mineral, recognized as a supergene mineral, red brown colour, 0.25 – 1 mm. Hematite replaced pyrite (Pl. 1C), marcasite, and sphalerite

Goethite: An oxide mineral with the size is 0.1-0.5 mm, subhedral-anhedral, grey colour and its occurrence to replace pyrite.

Malachite: It is a copper carbonate hydroxide mineral. Its appearance is identified at Wae-Satu, Tamilouw and adjacent to silica-carbonate alteration.

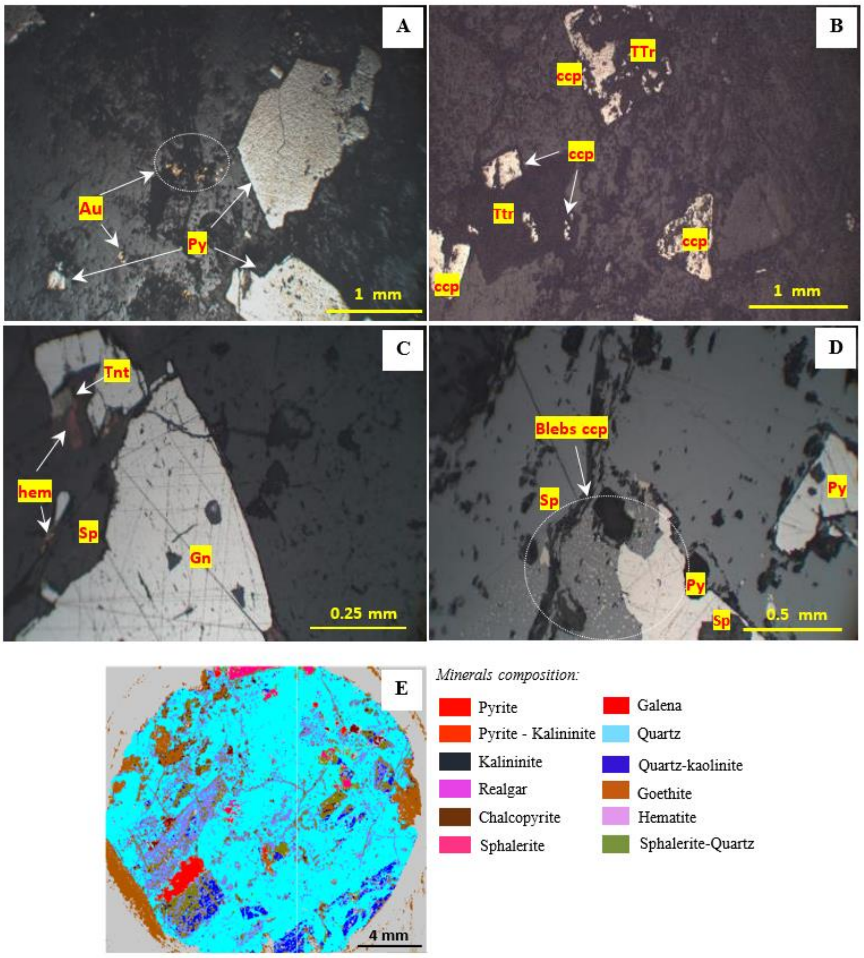

Plate (1): Photomicrographs showing ore minerals assemblage analysis at Tamilouw-Haya; (A) Disseminated texture of pyrite and "free gold grain" or independent gold within quartz gangue, (B) Replacement texture of tetrahedrite, indicating chalcopyrite is replaced by tetrahedrite, (C) Sphalerite and galena show intergrowth texture and hematite appear as Fe-oxide mineral replaces sphalerite and tennantite, (D) Chalcopyrite and sphalerite exsolution-texture, sphalerite replaces pyrite and disseminated texture of subhedral pyrite within quartz gangue, (E) Elemental mapping using micro-XRF showing distributions of pyrite, kalininite, realgar, sphalerite, chalcopyrite, galena, goethite and hematite. (Abbreviations: Au=gold, Sp=Sphalerite, Py=pyrite, Ttr=Tetrahedrite, Ccp=Chalcopyrite, Tnt=tennantite, Gn=Galena, Cov=covellite, Hem=hematite).

(B) Paragenetic sequence

Microscope observation and elemental mapping using Micro-XRF are used to interpret mutual relationship among minerals and their assemblage. The paragenetic sequence is obviously inferred from these interpretation and observation. Ore textures at Tamilouw-Haya show disseminated texture, simultaneous crystallization (intergrowth), inclusions, replacements and exolutions-decomposition textures. Ore minerals and gangue paragenetic sequence from epizonal – mesozonal orogenic gold deposit at Tamilouw – Haya are shown in Table (1).

Table (1): Paragenetic stage of mineralized veins at Tamilouw – Haya.

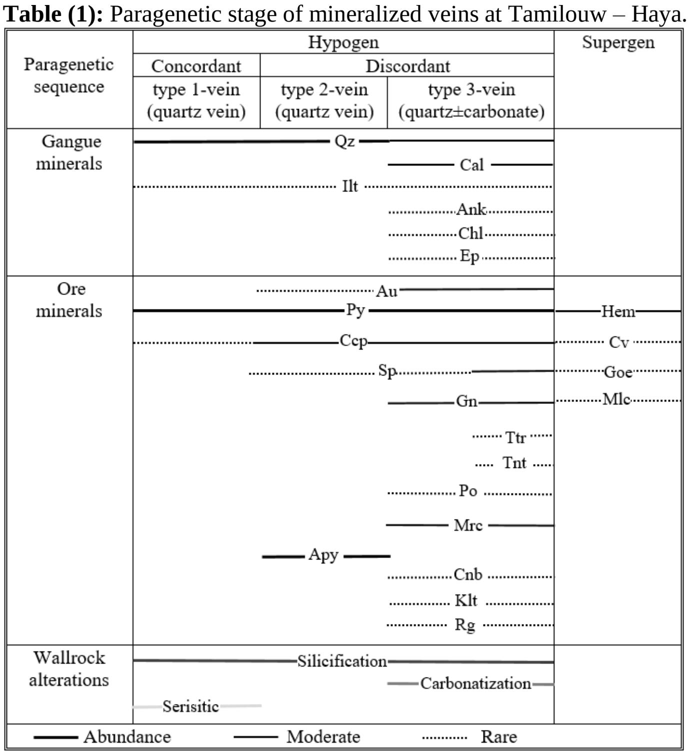

(Abbreviations : Qz : Quartz, Cal : Calcite, ilt : illite, Py : Pyrite, Au : Native gold, Ccp : Chalcopyrite, Sp : Sphalerite, Gn:Galena, Po : Pyrrhotite, Ttr : tetrahedrite, Tnt : tennantite, Mrc : Marcasite, Apy, Arsenopyrite, Cnb : cinnabar, Hem : Hematite, Cv : Covellite, Mlc : malachite, Goe : goethite)

Disseminated texture is found in almost all vein sample types, consisting of ore minerals from various type minerals such as pyrite, chalcopyrite and sphalerite, but mostly often found in pyrite. Gold dissemination is also found as “free gold grain”. The gold paragenetic sequence against other ore minerals is unable to be determined yet, but it is assumed that the process of its formation coincides with ore minerals formation in the disseminated texture.

Simultaneous or intergrowth crystallization textures are occurred in both galena and sphalerite as well as chalcopyrite and galena. These showed paragenetic relationship between galena, sphalerite and chalcopyrite, are simultaneously formed or at the same time of deposition. Replacement textures are formed in chalcopyrite and sphalerite minerals as well as tennantite and galena which are replaced by hematite and covellite minerals. Additionally, chalcopyrite is also replaced by tetrahedrite. Replacement minerals paragenesis indicates its formation at the end of ore deposition.

The ex-decomposition texture found was "chalcopyrite disease" (Barton and Betkhe, 1987); it was formed by blebs or chalcopyrite mineral emulsion/inclusions in the sphalerite which showed chalcopyrite formed at earlier time. Kalogeropoulos (1982) stated chalcopyrite disease is a cancerous replacement produced by reacting FeS in sphalerite with Cu in aqueous solution. In general, sphalerite is formed as late stage than other sulfide minerals such as chalcopyrite and galena. Covellite, hematite, goethite and malachite are supergene minerals; formed in the end of mineralization.

(C) Mineral Chemistry

Minor Elements in Pyrite from Tamilouw – Haya deposit:

The most abundant sulphide mineral at Haya – Tamilouw epizonal - mesozonal orogenic gold is pyrite. This Fe-sulphide fills altered metapelitic to slate wallrocks as vein/veinlets and reflecting euhedral to subhedral shape within quartz gangue in ore microscopy. In this research, SEM – EDS and Micro-XRF are used to describe elemental mapping and elements composition contained in pyrite. The SEM – EDS and Micro-XRF results reveal that nearly all pyrite samples contain a significant amounts and a wide range of other minor elements such as Co, Ni, Cd, Au, Ag and As (Tab. 2).

Elements including Se and Te are under detection limit or absent and might indicate that deposit is not associated with low sulfidation epithermal and igneous rocks or intrusion-related deposit. High concentrate of Se and Te is related to igneous rock, low sulfidation epithermal and Carlin – type deposit (Keith *et al*., 2018; Shao *et al*., 2018).

There were twelve data of shoot points within pyrite field from 3 alteration types to investigate its elemental composition for analysis. Pyrite from sericitic alteration shows its average minor elements as follows: Cd (0.12-0.20 wt. %), Co (0.12-0.39 wt.%), Ni (0.06-0.22 wt.%), Ag (<0.01-0.01 wt.%), Au (2.01-4.59 wt.%) and As (0.26-0.39 wt.%). Pyrite from carbonatization alteration shows a slightly different of its minor elements composition with their composition are Cd (0.06-0.18 wt. %), Co (0.18-0.36 wt.%), Ni (0.07-0.14 wt.%), Ag (<0.01-0.08 wt.%), Au (0.12-0.26 wt.%) and As (0.05-0.17wt.%). Comparison of pyrite from sericitic and carbonatization, pyrite from silicification alteration shows its average minor elements are Cd (<0.01-0.26 wt. %), Co (0.13-0.32 wt. %), Ni (0.05-0.17 wt.%), Ag (0.01-0.03 wt.%), Au (0.23-1.58 wt.%) and As (<0.01-0.14 wt.%). Overall, Co : Ni ratio from these 3 alteration types are 0.33-3.25 wt.%, 1.57-5.34 wt.% and 0.12-2.77 wt.%, respectively (Tab. 2).

Table (2): Mineral chemistry of pyrite using SEM-EDS and Micro-XRF (wt.%)

Sample code	Major elements		Minor elements								
	Fe	S	Ag	Au	Cd	As	Co	Ni	Se	Te	Co: Ni
Sericitic alteration :											
Tmw-Lt.18.1*	41.70	52.94	0.01	4.59	0.20	0.39	0.12	0.06	<0.01	<0.01	2.00
Tmw-Lt.18.2*	43.62	51.94	<0.01	3.05	0.15	0.26	0.39	0.12	<0.01	<0.01	3.25
Tmw-Lt.18.3*	45.78	50.94	0.01	2.01	0.12	0.31	0.17	0.22	<0.01	<0.01	0.33
Carbonatization alteration :											
Tmw-Lt.1.1*	40.41	53.58	<0.01	0.26	0.06	0.05	0.36	0.08	<0.01	<0.01	4.50
Tmw-Lt.1.2*	42.75	52.64	<0.01	0.19	0.02	0.13	0.22	0.14	<0.01	<0.01	1.57
Tmw-Lt.1.3*	43.12	50.27	<0.01	0.12	0.18	0.05	0.18	0.07	<0.01	<0.01	2.57
Tmw-Lt.01 (avg)**	48.29	50.16	0.08	0.16	0.17	0.08	0.25	0.08	<0.01	<0.01	5.34
Tmw-Ylsi.06 (avg)**	49.70	48.88	<0.01	0.13	0.18	0.17	0.08	0.06	<0.01	<0.01	4.94
Silicification alteration :											
Hy-wnm.07.1*	40.82	50.37	0.03	1.58	0.08	<0.01	0.14	0.06	<0.01	<0.01	2.33
Hy-wnm.07.2*	41.35	52.37	0.01	0.24	0.01	0.14	0.19	0.17	<0.01	<0.01	0.12
Hy-wnm.07.3*	40.82	52.57	0.01	1.55	0.26	0.01	0.32	0.10	<0.01	<0.01	1.78
Hy-Wyu.02 (Avg)**	49.05	48.40	0.01	0.23	<0.01	0.38	0.13	0.05	<0.01	<0.01	2.77
Average	43.95	51.25	0.02	1.18	0.13	0.18	0.21	0.10	<0.01	<0.01	2.86

Note: * SEM-EDS analyses
** Micro-XRF analyses
< 0.01 is lower detection

The SEM-EDS and Micro-XRF results show a well-defined negative correlation between As and S (Tab.3) which is consistent with the substitution of As for S as anionic As^{-} in the Fe $(S_{1-x}As_{x})_{2}$ solid solution in reducing environments (Fleet and Mumin, 1997; Reich *et al.*, 2005).

Xuexin (1984) revealed that the Co : Ni ratios for pyrites from various ores have been calculated and counted and it is not hard to come for the final conclusions (Tab. 4). All the Co: Ni ratios for sedimentary pyrites are lower than 0.8. The Co: Ni ratios for volcanogenic massive pyrites are higher than 3.5 and The Co:Ni ratios for volcano-hydrothermal, metamorphosed and skarn-hydrothermal pyrites are in the range of 2-3. Despite the effect of temperature was slight influenced, it is notable that pyrite from high-temperature deposit is generally high in cobalt but Ni content does not show a significant signature (Co > Ni).

Table (3): Pairs correlation of S, As, Co, Ni, and Fe elements within pyrite field from the Tamilouw – Haya deposit.

	S	*As*	*Co*	*Ni*	*Fe*
S	1				
As	-0,162755	1			
Co	0,584518	-0,327165	1		
Ni	0,333405	0,144819	0,183612	1	
Fe	-0,817132	0,398707	-0,409308	-0,149354	1

Table (4): Type of pyrite based on Co: Ni ratio classified by Xuexin (1984)

Type of pyrite	Co	Ni	Co : Ni
Sedimentary-type	41	65	0.8
Volcano-hydrotermal, metamorphosed and skarn-hydroternal – type	141	121	2 - 3
Volcangenic massive sulphide – type	486	56	3.5
Tamilouw – Haya (Researched area)	2110	1000	2.86

For this conclusion, it is deal with the average result of pyrite at Tamilouw – Haya that show Co: Ni is 2.86. The Co: Ni ratios for Tamilouw - Haya pyrites are higher than those for sedimentary pyrites, lower than those for volcanogenic massive pyrites and similar to those for the slightly volcano-hydrothermal, metamorphosed and skarn hydrothermal type.

Minor Elements in Galena from Tamilouw – Haya deposit:

Twelve spot representatives for galena analysis from Tamilouw – Haya deposit were analyzed for Fe, Hg, Sb, Ag, Au, Bi and Se using SEM-EDS and Micro-XRF (Tab.5). This table showed that the Hg contents are very low (0.01-0.28wt.%) to below detection limit (< 0.01wt.%).

Table (5): Mineral chemistry of galena using SEM-EDS and Micro-XRF (wt.%)

Sample code	Major elements		Minor elements						
	Pb	S	Hg	Sb	Bi	Fe	Ag	Au	Se
Tmw-ylsi.6.1**	83.56	14.49	<0.01	<0.01	<0.01	<0.01	<0.01	<0.01	<0.01
Tmw-ylsi.6.2**	82.33	14.36	<0.01	<0.01	<0.01	0.28	<0.01	<0.01	<0.01
Tmw-ylsi.6.4**	85.54	13.60	<0.01	<0.01	<0.01	0.86	<0.01	<0.01	<0.01
Tmw-ylsi.6.5**	88.99	9.16	<0.01	<0.01	<0.01	0.46	<0.01	<0.01	<0.01
Tmw-ylsi.6.6**	86.76	10.76	<0.01	<0.01	<0.01	0.23	0.31	<0.01	<0.01
Tmw-ylsi.6.7**	88.30	9.33	<0.01	<0.01	<0.01	0.17	<0.01	<0.01	<0.01
Tmw-ylsi.6.8**	88.17	7.20	0.28	<0.01	<0.01	0.48	0.23	<0.01	<0.01
Tmw-ylsi.6.9**	84.75	6.09	<0.01	<0.01	<0.01	0.38	<0.01	<0.01	<0.01
Tmw-ylsi.6.10**	66.73	7.14	<0.01	<0.01	<0.01	0.30	<0.01	<0.01	<0.01
Hy-Wnm.7.1*	74.82	9.08	0.01	<0.01	<0.01	1.68	0.18	3.2	<0.01
Hy-Wnm.7.2*	73.34	11.38	<0.01	<0.01	<0.01	3.31	0.12	2.58	0.01
Hy-Wnm.7.3*	75.89	11.06	0.01	<0.01	<0.01	1.24	0.14	2.57	0.01
Average	81.60	10.30	0.10	<0.01	<0.01	0.85	0.20	2.78	0.01

Note: SEM-EDX analyses*
*** Micro-XRF analyses*
< 0.01 is below detection limit

The Se, Au and Fe contents are extremely low and in the ranges less than 0.01 wt.%, 3.2 wt.% and 3.31 wt.%, respectively. Sb, Ag, and Bi are generally used to demonstrate ore-forming temperature of galena. Foord and Shawe (1989) discussed the crystallochemical relationships of Ag, Sb and Bi with galena and this can be explained by the coupled substitution between them as follow: $Ag^{+} + Sb^{3+}(Bi^{3+}) \leftrightarrow 2Pb^{2+}$

Fleischer (1955) stated that the content of Ag, Bi and Sb declined with decreasing temperature of formation. The presence of bismuth (Bi) itself in galena is indication of high temperature magma-near deposits (Schroll, 1955). In addition, the examined Bi-bearing galena are relatively high-temperature which agrees with the experimental data for arising of such solid solutions (Bonev, 2007). At Tamilouw – Haya deposit, galena shows the Ag, Sb and Bi contents are very low to below detection limit with slightly variation. Ag is within the ranges < 0.01–0.31 wt.% (average 0.20 wt.%), Sb and Bi are below detection limit (<0.01 wt.%). Although Galena is an Ag- carrier, it seems like galena in Tamilouw – Haya is non-argentiferous galena. The best sample for non-argentiferous galena is able to found in Alanish Locality, Northern Iraq (Awadh and Nejbert, 2016). Therefore, it can be inferred that galena from Tamilouw - Haya deposit may be formed in low temperature.

Minor Elements in Sphalerite from Tamilouw – Haya deposit :

Sphalerite composed of Zn and S atoms arranged in a tetrahedral coordination within a face-centred cubic lattice (Lockington *et al.*, 2014). Sphalerite is the main ore for zinc and the dominant mineral in most types of zinc sulphide deposits. In this study, SEM-EDX and Micro-XRF are used to analyze 12 spot representatives of sphalerite samples from Tamilouw-Haya orogenic deposit. Some detected of minor elements contained in sphalerite are Ga, Ge, Cd, Fe, Ag and Au. The results are listed in Table (6).

Table (6): Elements of sphalerite using SEM-EDS and Micro-XRF (wt.%)

Sample code	Major elements		Minor elements						Results		
	Zn	S	Ga	Ge	Cd	Fe	Ag	Au	Zn/Cd	Ga/Ge	Log Ga/Ge
Hy-wnm.07.1*	60.27	32.14	0.90	0.04	0.06	5.48	0.13	<0.01	1004.5	22.50	1.35
Hy-wnm.07.2*	61.58	30.43	1.87	0.02	<0.01	5.74	0.05	<0.01	6158	93.50	1.97
Hy-wnm.07.3*	59.54	31.46	1.85	0.41	0.19	4.92	0.10	<0.01	313.37	4.51	0.65
Tmw-Ws.03.1*	56.37	32.4	0.63	0.03	<0.01	7.88	0.24	<0.01	5637	21.00	1.32
Tmw-Ws.03.2*	57.83	30.62	1.57	0.12	0.22	6.38	<0.01	<0.01	262.86	13.08	1.12
Tmw-Ws.03.3*	56.02	30.40	1.87	0.01	<0.01	8.83	0.01	<0.01	5602	187.02	2.27
Tmw-Ylsi6.1**	64.88	19.72	0.61	0.02	<0.01	14.82	<0.01	<0.01	6488	30.50	1.48
Tmw-Ylsi6.2**	61.62	27.37	0.57	0.13	<0.01	9.53	<0.01	<0.01	6162	4.38	0.64
Tmw-Ylsi6.3**	57.84	26.22	0.40	0.24	<0.01	14.92	0.12	<0.01	5784	1.67	0.22
Tmw-Ylsi6.9**	58.8	28.22	0.50	0.22	0.18	11.06	<0.01	<0.01	326.67	2.27	0.36
Tmw-Ylsi6.10**	60.23	29.65	0.58	0.13	<0.01	9.19	<0.01	<0.01	6023	4.46	0.65
Tmw-Ylsi6.11**	58.94	29.02	0.62	0.05	<0.01	11.18	<0.01	<0.01	5894	12.4	1.09
Average	59.49	28.97	0.99	0.12	0.06	9.16	0.06	0.01	4137.95	33.11	1.09

*Note: * SEM-EDX analyses*
*** Micro-XRF analyses*
< 0.01 is lower detection

This table shows that Tamilouw – Haya sphalerites hardly contain Fe which is in the range of 4.92-14.92 wt.%.. The Cd contents range from 0.06 wt. % to 0.22 wt.% of which a half of them are below detection limit (<0.01wt.%). The Ga, Ge, and Ag contents are within the ranges 0.4-1.87wt.%, <0.01 - 0.41 wt.%, and <0.01 - 0.24 wt.%, respectively. Nearly all researchers agreed that sphalerite from low temperature deposits such as those of the

Mississippi Valley type tend to be higher in germanium content than those from mesothermal or high temperature deposits (Warren and Thompson, 1945), but many exceptions were noted. The data of Moller (1985) showed practically that Ga/Ge ratio will imply to temperature of ore formation. If the Ga concentration is higher than Ge, it may indicate of high temperature deposits. In this case, the maximum content of gallium (Ga) in sphalerite at Tamilouw – Haya deposit achieved 1.87 wt. % and it means that the deposit occurred under high-temperature formation.

Jonasson and Sangster (1978) concluded that the Cd contents and Zn/Cd ratios in sphalerites vary with the genetic types of deposit and the metallogenetic epochs. The classification of ore-deposit type is distinguished by observing some sulphide ores in Canada. This classification is described as follows:

1. The Cd contents in sphalerites from volcano-sedimentary type deposits and Alpine type deposits are the lowest in all of the discussed deposits or districts with their Zn/Cd ratios are 417-531.
2. The Cd contents in sphalerites from metamorphosed sedimentary deposits and carbonate-hosted strata-bound and stratiform deposits are medium, show their Zn/Cd ratios are 252-330.
3. The Cd contents in sphalerites from hydrothermal deposits (including volcano-hydrothermal deposits) and skarn-hydrothermal deposits are the highest with their Zn/Cd ratios are 104-214.

Since a half of Cd contents of sphalerite are below of detection but the Zn contents are the highest presence in the investigated area, therefore Zn:Cd ratios are incomparable with this classification. They show a significance of very high Zn/Cd ratios (262.86 - 6488, average= 4137.95) due to very low of Cd contents.

(D) Geothermometry (Ga/Ge) Sphalerite

Moller (1985) used geothermometry (Ga/Ge) sphalerite to determine temperatures in the source region of ore solutions to estimate mixing degree of the ore fluid. The combination of (Ga/Ge) sphalerite and homogenization temperature will assist in evaluating ore forming process. In this study, Geothermometry (Ga/Ge) sphalerite analysis at Tamilouw – Haya using SEM-EDS and Micro-XRF presented in Table (6).

Based on Table 6, the average of germanium (Ge) content is 0.12 wt.% in sphalerite. In addition, the value of gallium (Ga) in the sample shows a range of 0.4 to 1.87 wt.% with an average of this element is 0.99 wt.%. This shows that sphalerite in the study area tends to be formed in relatively high temperature conditions. Moreover, the iron (Fe) content in sphalerite reaches 14.92 wt.% which may support and indicates that the temperature of ore formation is relatively a high temperature. The iron content generally increases with increasing formation temperature and can reach up to 40% in sphalerite (Nesse, 2013).

From the results of the log Ga/Ge calculation at Tamilouw-Haya deposit, the maximum value is 2.27, while the minimum value shows a value of 0.22. Based on geothermometry

(Ga/Ge) analysis of sphalerite which is then plotted on the equilibrium feldspar-mica-quartz graph and comparing with pressure and depth, the value of homogenization temperature (T_h) shows temperature ranging from 210-305° C (Diag. 1).

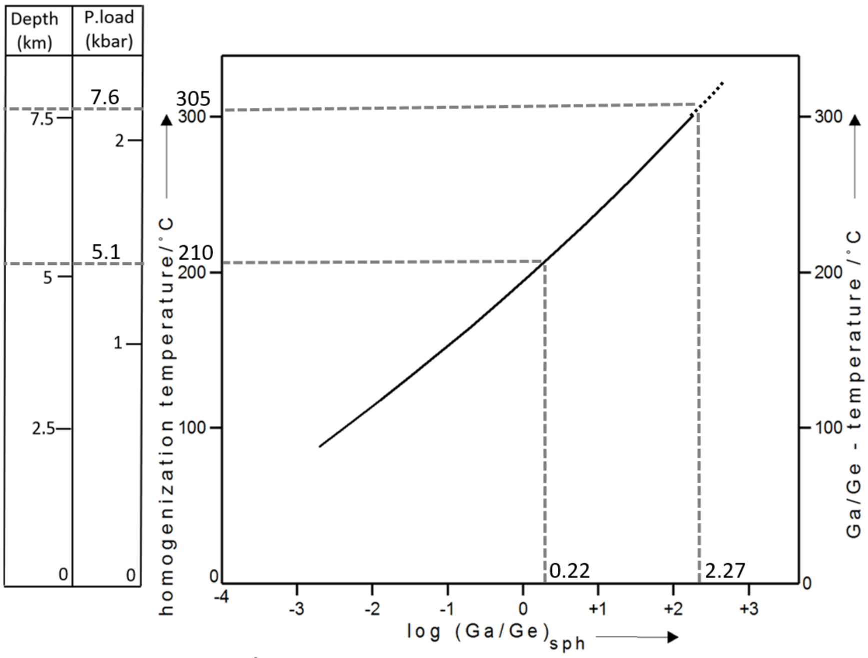

Diagram (1): Graph of homogenization temperature (T_h) based on log geotermometry (Ga/Ge) sphalerite (Moller, 1985). P. load and depth is obtained from Australian continuum model correlation (modified after Groves, 1993; Groves *et al.*, 1998; Gebre-Mariam *et al.*, 1995; Goldfarb and Groves, 2015).

CONCLUSIONS

Minerals assemblage at Tamilouw – Haya are native gold, chalcopyrite, pyrite, sphalerite, galena, pyrrhotite, marcasite, realgar, kalininite, arsenopyrite, minor sulfosalts (tetrahedrite-tennantite), covellite, hematite, goethite and malachite. There are 6 main prospects of gold mineralization in the researched area namely Wae Lata, Wae Nama, Wae Satu, Wae Yala, Wae Namasula and Way Wayaudara. High-grade gold ores in this area are generally found in quartz±carbonate veins (V_3) with the main alteration processes are silicification and carbonatization. The ore mineral textures are composed of disseminated, exsolution-decomposition, simultaneous crystallization (intergrowth) and replacement.

The paragenesis deciphered that quartz, calcite, ankerite, siderite, illite, chlorite and epidote were gangue minerals and ore mineralization are embedded within 3 types of quartz/quartz carbonate veins. Pyrite field in Tamilouw - Haya has cobalt content but Ni does not show a significant signature (Co > Ni) which means that the Tamilouw - Haya gold deposit was formed in relatively a high-temperature deposit. The Co/Ni ratios for Tamilouw – Haya pyrites are higher than those for sedimentary pyrites, lower than those for volcanogenic and skarn-hydrothermal pyrites, and more similar to those for the volcano-hydrothermal, metamorphosed and skarn hydrothermal type. Furthermore, the enrichment of cobalt, nickel and arsenic in pyrite indicates that these elements are available during certain metamorphic phases. Galena is characterized by below detection limit of Sb and Bi elements, while the Ag contents are relatively low, so it can be concluded that galena from the Tamilouw - Haya deposit was formed at decreasing temperature.

The minor elements of sphalerite in Tamilouw-Haya shows the element of Ga > Ge and increasing of Fe content which indicates the formation of sphalerite at a relatively high temperature. Moreover, the Ga/Ge sphalerite microtermometry has an elevated homogenization temperature (T_h) ranging from 210^o-305^o C.

ACKNOWLEDGEMENTS

This paper is written in frame of the first author in doctoral program at Universitas Gadjah Mada. I would like to thank local government of Maluku and LPDP for doctoral Scholarship sponsor. Their help is thankfully appreciated. A deep gratitude goes to Geology Department of Energy and Mineral Resources of Maluku and Okki Verdiansyah who assist me during my field work and data processing. My special thanks to Dr.Eng Zain Tuakia and Dr. Hasria for personal sharing and guidance.

LITERATURE CITED

Audley-Charles, M. G., Carter, D. J., Barber, A. J., Norvick, M. S. and Tjokrosapoetro, S. 1979. Re-interpretation of the Geology of Seram : Implications for the Banda Arcs and Northern Australia. *Journal of Geology Society of London*, 136: 547-568.

Awadh, S. M. and Nejbert, K. 2016. Polymetallic sulfide ores hosted in Late Permian carbonate at the Alanish locality, northern Iraq: petrography and mineral chemistry. Arabian Journal of Geosciences, 9:1-15.

Barton, P. B. and Bethke, P. M. 1987. Chalcopyrite disease in sphalerite: pathology and epidemiology. *American Mineralogist*, 72 (5-6): 451-467.

Bonev, I. K. 2007. Crystal habit of Ag-, Sb- and Bi-bearing galena from the Pb-Zn ore deposits in the Rhodope Mountains. *Geochemistry, Mineralogy and Petrology*, 45: 1-18.

Bierlein, F. P., Hughes, M., Dunphy, J., McKnight, S., Reynolds, P. R. and Waldron, H. M. 2001. Trace element geochemistry, ^{40}Ar/^{39}Ar ages, Sm–Ndsystematics and tectonic implications of mafic-intermediate dykes associated with orogenic lode gold mineralisation in central Victoria, Australia. *Lithos*, 58: 1-31.

Craig, J. R. 2001. Ore-mineral textures and the tales they tell. *The Canadian Mineralogist*, 39 (4): 937–956.

Fleet, M. E. and Mumin, A. H. 1997. Gold-bearing arsenian pyrite, marcasite and arsenopyrite from Carlin Trend gold deposits and laboratory synthesis. *American Mineralogist*, 82: 182–193.

Fleischer, M. 1955. Minor elements in some silfide minerals. Economic Geology, 50th Anniversary Volume, p. 970–1024.

Foord, E. E. and Shawe, D. R. 1989. The Pb-Bi-Ag-Cu-(Hg) chemistry of galena and some associated sulfosalts: a review and some new data from Colorado, California and Pennsylvania. *Canadian Mineralogist*, 27:363–382.

Franklin, Moetamar and Reza, M. 2013. Inventarisasi endapan logam di Kabupaten Seram Bagian Barat Provinsi Maluku. *Laporan internal*. Tidak dipublikasikan. Pusat Sumber Daya Geologi, Bandung, 125 pp. (In Indonesian).

Gebre-Mariam, M., Hagemann, S. G. and Groves, D.I. 1995. A classification scheme for epigenetic Archaean lode-gold deposits. *Mineral Deposita,* 30: 408–410.

Goldfarb, R. J. and Groves, D. I. 2015. Orogenic gold : Common or evolving fluid and metal sources through time. *Lithos*, 233: 2-26

Goldfarb, R. J., Groves D. I. and Gardoll, S. 2001.Orogenic gold and geologic time: a global synthesis. *Ore Geology Review*, 18: 1-75.

Goldfarb, R. J., Baker, T., Dubé, B., Groves, D. I., Hart, C. J. R. and Gosselin, P. 2005. Distribution, character, and genesis of gold deposits in metamorphic terranes, *In*: Hedenquist, J. W., Thompson, J. F. H., Goldfarb, R. J. and Richards, J. P. (eds). Economic geology: One Hundreth Anniversary Volume: Littleton, Colorado, Society of Economic Geologists, Inc., p. 407-450.

Groves, D. I. 1993. The crustal continuum model for late-Archean lode gold deposits of the Yilgarn block, Western Australia. *Mineral Deposita*, 28:366-374

Groves, D. I., Goldfarb, R. J., Gebre M. M., Hageman,S. G. and Robert, F. 1998. Orogenic gold deposit; A proposed classification in the context of their crustal distribution and relationship to other gold deposits types. *Ore Geology Review*, 13: 7-27.

Hamilton, W. B. 1979. Tectonics of the Indonesian region. U.S.Geological Survey Professional Paper, no. 1078, U.S. Govt. Print. Off., 345pp.

Hasria. 2018. Karakteristik mineralisasi emas hidrotermal yang berasosiasi dengan batuan metamorf di Pegunungan Mendoke dan Rumbia pada lengan tenggara Pulau Sulawesi, Indonesia. *Ph.D. thesis*. Universitas Gadjah Mada, Yogyakarta, 281pp. (In Indonesian)

Idrus, A. and Prihatmoko, S. 2011. The metamorphic rock-hosted gold mineralization at Bombana, Southeast Sulawesi: a new exploration target in Indonesia, Proceedings of The Sulawesi Mineral Seminar, 28–29 Nov 2011, Manado, North Sulawesi, Indonesia, p. 243-258.

Idrus, A., Prihatmoko, S., Hartono, H. G., Idrus, F., Ernowo., Franklin, Moetamar and Setiawan, I. 2014. Some Key Features and Possible Origin of the Metamorphic Rock-Hosted Gold Mineralization in Buru Island, Indonesia. *Indonesian Journal on geoscience*,1(1): 9-19.

Jonasson, I.R. and Sangster, D.F. 1978. Zn/Cd ratios for sphalerites separated from some Canadian sulphide ore samples. *Paper-Geology Survey of Canada*, 78-1B: 195–201.

Kalogeropoulos, S.I.,1982. Chemical sediments in the hanging wall of volcanogenic massive sulfide deposits. Ph.D. thesis, Univ. Toronto, 488 pp.

Keith, M., Smith, J. D., Jenkin, R. T. G., Holwell, A. D. and Dye, D. M. 2018. A review of Te and Se systematics in hydrothermal pyrite from precious metal deposits: insights into ore-forming processes. *Ore Geology Review*, 96: 269-282.

Kemp, G. and Mogg, W. 1992. A reappraisal of the geology, tectonicsand prospectivity of Seram Island, Eastern Indonesia. *Proceedings of Indonesian Petroleum Association*, 21: 521–552.

Linthout, K., Helmers, H., Sopaheluwakan, J. and Nila, E. S. 1989. Metamorphic complexes in Buru and Seram, northern Banda Arc. *Netherlands Journal of Sea Research*, 24 (2-3): 345-356.

Lockington, J, A., Cook, N.J. and Ciobanu, L. C. 2014. Trace and minor elements in sphalerite from metamorphosed sulphide deposits. *Mineralogy and Petrology*, 108; 873-890.

Moller, P. 1985. Development and application of the Ga/Ge-Geothermometer for sphalerite from sediment hosted deposits. *In*: Germann, K. (ed.), Geochemical aspects for ore formation in recent and fossil sedimentary Environments, 15–30. Gebürder Borntraegerm Berlin.

Nesse, W. D. 2013. Introduction to optical mineralogy (4th ed.). New York: Oxford University Press. p 121

Powell, D. E. 1976. The geological evolution of the continental margin of Northwest Australia. *Journal of Australian Petroleum Exploration Association*, 10: 13-23.

Pownall, J. M., Hall, R. and Watkinson, I. M. 2013. Extreme extension across Seram and Ambon, eastern Indonesia: evidence for Banda slab rollback. *Solid Earth*, 4: 277–314.

Querubin, C. D. and Walters, S. 2011. Geology and mineralization of Awak mas: a sedimentary hosted gold deposit, South Sulawesi, Indonesia. Proceedings of The Sulawesi Mineral Seminar, 28–29 Nov 2011, Manado, North Sulawesi, Indonesia, p. 211–222.

Reich, M., Kesler, S. E., Utsunomiya, S., Palenik, C. S., Chryssoulis, S. L. and Ewing, R. C. 2005. Solubility of gold in arsenian pyrite. *Geochimica et Cosmochimica Acta*, 9: 2781–2796.

Schroll, E. 1955. Uber das Vorkommen einiger Spurenmetalle in Blei-Zink-Erzen der ostalpinen Metallprovinz, Tshermaks Mineralog, *Petrog*, 5:183–208. (In Germany)

Setyawan, B. W., Wijaya, B. and Guntoro, A. 2000. Mengurai Perkembangan Tektonik Pulau Seram dan Ambon. Prosiding IAGI 29th Annual Convention, 4:33-45. (In Indonesian)

Shao, J. Y., Wang, S. W., Liu, Q. Q. and Zhang, Y. 2018. Trace element analysis of pyrite from the Zhengchong gold deposit, Northeast Hunan province, China: Implications for the ore – forming process. *Minerals*, 8(6): 262.

Tjokrosapoetro, S. and Budhitrisna, T., 1982. Geology and tectonics of the northern Banda Arc. *Bulletin of the Indonesian Geological Research and Development Centre*, 6: 1-17.

Tjokrosapoetro, S., Achdan, A., Suwitodirdjo, S., Rusmana, E. and Abidin, H. Z. 1993. Pemetaan Geologi lembar Masohi sekala 1: 250.000. Pusat Penelitian dan Pengembangan Geologi, Bandung. (In Indonesian)

Valk, W. 1945. Contributions to the geology of West Seran. *In*: Rutten, L. and Hotz, W. (eds.), Geological, petrographical, and palaeontological results of explorations, carried out from September 1917 till June 1919 in the island of Ceram. De Bussy, Amsterdam, 104 pp.

Veevers, J. J. 1982. Western and northwestern margins of Australia. *In*: Nairn, A. E. M. and Stehli, F. .Oceanic Basin, p. 513-544.

Wajdi, M. F., Santoso, S. B., Kusumanto, D. and Digdowirogo, S. 2011. Metamorphic hosted low sulphidation epithermal gold system at Poboya, Central Sulawesi: a general descriptive review. Proceedings of the Sulawesi Mineral Seminar, 28–29 Nov 2011, Manado, North Sulawesi, Indonesia, p. 201–210.

Warren, H. V. and Thompson, R. M. 1945. Sphalerites from western Canada. *Economic Geology*, 40: 309-335.

Xuexin, S.1984. Minor Elements and Ore Genesis of the Fankou Lead-Zinc Deposit, China. *Mineral Deposita*, 19: 95–104.

Bull. Iraq nat. Hist. Mus.
(2021) 16 (3): 301- 323.

نشأة الخام والعناصر الثانوية لترسبات الذهب البنيوي في تاميلو هايا، جزيرة سيرام، إندونيسيا

هيرفين سماليهو*، عارفودين ادروس**، نوگروهو إمام سيتيوان** و
اي جيدي سوكادانا ***
*وكالة الطاقة والثروة المعدنية، مقاطعة مالوكو، إندونيسيا
**قسم الهندسة الجيولوجية، جامعة جادجا مادا، يوجياكارتا، إندونيسيا
*** الوكالة الوطنية للطاقة الذرية، إندونيسيا

تأريخ الاستلام: 2021/03/05، تأريخ القبول: 2021/04/30، تأريخ النشر: 2021/6/20

الخلاصة

تكونت ترسبات الذهب البنيوي في تاميلو هايا ضمن معقد صخور تيهورو المتحولة وصخور السليت (الاردواز). يتشكل تمعدن الذهب والكبريتيدات المتعددة الفلزات في منطقة الدراسة في الغالب في شكل عروق ومخزون وبريشيا على الرغم من أن الانتشار الطفيف ظهر بشكل طفيف في عينات الصخور العائمة. تم حصرها والتحكم فيها بواسطة تراكيب جيولوجية باتجاة NE-SW وNNE-SSW خلال عملية تكون المنشأ البنائية في أواخر العصر الميوسين إلى البليوسين.

يهيمن الذهب الخام في مجاميع الخامات المعدنية الشائعة في ترسبات تاميلو هايا اضافة الى الجالكوبايرايت، البايريت، السفاليريت، الجالينا، البيروتيت، رباعي الهيدريت-تينانتيت (سلفوسالت)، ماركاسايت، ريجار، كالينينايت وأرسينوبيريت، كمعادن الهيبوجين وتكون مصاحبة الى الكوفيلايت و هيماتيت، والجيوثايت، والملاخايت كمعادن سوبرجينية.

ان دراسة نشأة الخام و العناصر الثانوية للبيريت والجالينا والسفاليريت في تاميلو – هايا، تم باستخدام ثلاثة طرق. استخدمت 46 عينة للتحليل

المجهري للخامات و 10 عينات لتحليلاتSEM-EDX المجهر الالكتروني الماسح والاشعة السينية Micro-XRFلتفسير العلاقة المتبادلة وتسلسل نشاتها. لقد اظهر النسيج المعدني للخام القوام المنتشر، و التبلور المتزامن (النمو الداخلي) ، والشوائب، والاحلال، وتاثير المحاليل البنائي والتهدمي للنسيج.

متوسط محتوى Co هو 0.21٪ بالوزن و ٪0.10 Ni بالوزن مما قد يعكس نسبة Co:Ni هي 2.86 في البيريت؛ و هذا يعني أن محتوى Co أعلى من Ni ويشير إلى أن أصل البيريت قد يكون مرتبطًا بالنوع البركاني الحراري المائي والمتحول والنوع الحراري المائي.

بالمقارنة مع البيريت، يظهر متوسط محتويات العناصر الثانوية في sphaleriteمحتوى Fe هو 9.16 بالوزن٪، Ga هو 0.99 بالوزن٪ ، Ge هو 0.12 بالوزن٪ ولوغار Ga / Geيتراوح من <0.36 إلى 2.27 بالوزن٪. علاوة على ذلك ، يظهر متوسط محتويات المعادن الثمينة داخل galenaأن محتوى Au هو <0.01 - 2.78٪ بالوزن و Ag هو 0.12-0.31٪ بالوزن. استنادًا إلى الأوصاف السابقة للمحتوى العالي من الحديد في البيريت والسباليريت، فإن Ga> Ge ، Co> Ni في البيريت، يشير المحتوى المنخفض من Ag فيGalena إلى أن البيريت والجالينا والسفاليريت من تاميلو-هايا تشكلت تحت ظروف درجة حرارة عالية إلى معتدلة في عمق 5.1- 7.6 كم من paleodepth .